Study of Epithermal-Neutron Spectrum Variation versus Depth in Water Phantoms

(Article begins on next page)

17 October 2023

Study of Epithermal-Neutron Spectrum Variation Versus Depth in Water Phantoms

Grazia Gambarini[1,2], **Daniela Bettega**[1,2], **Andrea Gebbia**[1], **Emanuele Artuso**[1], **Marco Felisi**[1], **Dario Giove**[1,2], **Elisabetta Durisi**[3,4], **Valeria Monti**[3,4], **Vit Klupak**[5], **Ladislav Viererbl**[5] and **Miroslav Vins**[5]

ABSTRACT

A study has been carried out concerning the energy spectrum of the epithermal beam designed for boron neutron capture therapy (BNCT) of the LVR-15 research reactor. MC calculations concerning radiation transport and dose distribution in water volumes of various shapes exposed to the epithermal neutron beam were developed with MCNP/MCNPX. In addition to the energy spectra at various depths in a water phantom, longitudinal and transversal profiles of the fluence of neutrons above and below the cadmium cut-off (0.5 eV) have been evaluated for different shapes of the phantom. In particular, significant differences were found in the spatial distribution of neutrons for energy E < 0.5 eV. In order to confirm the reliability of simulations, a few depth profiles of neutron fluence below 0.5 eV, evaluated by means of MC calculations, has been compared with the profile of thermal neutrons obtained by means of experimental measurements. The consistency of results is good.

Keywords

Epithermal neutron beam, energy spectrum, MCNP, water phantom, neutron fluence profile.

INTRODUCTION

Epithermal neutron transport in water or other tissue-equivalent (TE) materials is a challenging task because the neutron energy spectrum is not only a function of depth but also of the shape and dimension of the irradiated volume. In fact, epithermal neutrons in water are mainly moderated by the elastic scattering interactions with hydrogen nuclei $^1H(n,n)^1H$. The continuous increase of isotropy in the motion of neutrons as they slow down leads to backscattering effects and the spatial distribution of thermalized neutrons is consistently depend on the size and shape of the irradiated volume. Let us consider, for general assessments, the neutrons below and above the Cadmium cut-off (0.5 eV) that can briefly be called thermalized and non-thermalized respectively. The trend versus depth of the fluence of non-thermalized neutrons is an almost exponential decrease, not much depending on the shape and dimensions of the irradiated volume. In fact, along the axis of the beam, the differences are minimal; visible changes occur along directions away from this axis, mainly approaching the lateral boundary of the irradiated volume. On the contrary, significant variations can be found in all the volume, also along the beam axis, for thermalized neutrons.

From a dosimetric point of view, the variability of the spatial distribution of the thermalized component of the neutron beam causes consequences in the relative distribution of the various components of the absorbed dose. In water, the dose is basically due to recoil protons resulting from the elastic scattering interaction $^1H(n,n)^1H$ and from the 2.2 MeV photons generated in the reactions of thermal neutrons with hydrogen ($^1H(n,\gamma)^2H$, σ_{th} = 0.33 b). The contribution to the gamma dose given by the reactor background can be significant at the beginning of the irradiated volume but within a few centimeters becomes negligible with respect to the contribution of the 2.2 MeV photons. The reactor background will not be considered in this study. In the energy range of epithermal neutron beams, the dose from recoil protons can be considered as locally released in the interaction site, giving a spatial distribution similar to that of the non-thermalized neutrons, decreasing therefore with depth in the irradiated volume in a way not much dependent on its size. The problem of the gamma dose due to the 2.2 MeV photons is very different, because such photons release energy also in positions far from that of the reaction. One can idealize, in a rough approximation, a process by which each point of the medium is equivalent to a source of 2.2 MeV gammas having intensity proportional to the thermal neutron fluence at that position. Thus, a variation of shape or size of the irradiated volume that causes a variation of thermalized neutron fluence produces also a gamma dose change in the whole volume.

[1] Università degli Studi di Milano, Milano, 20133, Italy
[2] INFN Istituto Nazionale di Fisica Nucleare, Section of Milan, Milano, 20133, Italy
[3] Department of Physics, Università degli Studi di Torino, Torino, 10125, Italy
[4] INFN Istituto Nazionale di Fisica Nucleare, Section of Turin, Torino, 10125, Italy
[5] Department of Neutron Physics, Research Centre Řež, Czech Republic

CARRIED OUT EVALUATIONS
In this work, MC calculations concerning radiation transport and dose distribution in water volumes of various shapes exposed to the epithermal neutron beams were developed. The outcomes of all calculations are given for source particle. In a few cases, the results were compared with experimental measurements. In particular, the carried out studies concern the epithermal neutron beam of the LVR-15 research reactor, designed for boron neutron capture therapy (BNCT) at the Research Centre Řež (Czech Republic).

Simulations have been performed with MCNP/MCNPX, 2006. The radiation source file utilized in input of simulations is the same that was utilized in the 'pre-clinical trials' for the calculations of the patient treatment planning at LVR-15 reactor. The epithermal column mouth is circular, with a diameter of 12 cm.

Calculations were performed simulating water phantoms of four different geometries: two parallelepipeds with sides $40x40x20$ cm^3 and $14x14x20$ cm^3, a cube of 14 cm of side and a sphere of 16 cm in diameter. In-depth profiles have been evaluated along the beam axis, along directions at various distances from the beam axis and along transversal direction at various depths.

In order to attain the neutron spectra at the various depths in water, neutron fluence profiles along the beam axis have been calculated for a sequence of energy intervals in the range from 0.01 eV and 10 MeV. For each decade of energy, the neutron fluence profiles in 5 intervals of energy were evaluated. From these profiles, the energy spectra at various depths have been achieved.

The energy spectra have been carried out for the cubic water phantom of 14 cm of side. Various longitudinal and transversal profiles of neutron fluence below and above cadmium cut-off have been attained for all the phantoms and the results have been compared in order to highlight and quantify the differences. The evaluations have been focused mainly to the fluence of neutrons below the cadmium cut-off, because for energies > 0.5 eV no significant variations have been found.

RESULTS
Energy spectra
Initially, profiles with no phantom have been evaluated, in order to attain the neutron energy spectra at the collimator mouth and at a few distances from this. Then, the fluence profiles for the various selected energy intervals have been evaluated for the cubic water phantom of 14 cm of side, placed against the collimator mouth.

In Fig. 1, the neutron energy spectra at the center of the collimator mouth in absence and in presence of the water phantom are reported. Moreover, in the figure also the spectrum at a distance of 9 cm, without water phantom, is shown. We can see that in absence of water the spectrum displays a general fluence decrease, with no significant variation of the shape. On the contrary, the presence of a water phantom causes a remarkable growth of the neutron fluence which is much higher as the energy is less. This backscattering effect is particularly substantial under the cadmium cut-off. In Fig. 2, two transversal profiles of the thermalized neutron fluence, along a diameter of the collimator's mouth, are reported: the lower profile is the fluence without any phantom and the other one is that at the entrance of the large water phantom ($40x40x20$ cm^3) placed against the collimator.

In the water phantom, the fluence below the cut-off energy has shown to continuously increase up to a depth of 2.1 cm, with a continuous fluence decrease for the highest energies. After 2.1 cm of depth, the fluence decreases for all energies. For better visibility, in Fig. 3 the fluence spectra at depths from 0 cm to 2.1 cm are shown and in the insert of the same figure a few spectra from the same depth of 2.1 cm up to 9 cm are reported. With increasing depth, the statistical error of results increases and then the profiles show higher dispersion of data.

Neutron fluence and gamma dose profiles in different water phantoms
In order to investigate the variation in neutron transport resulting from differences in the shape and dimension of the irradiated volume, various profiles of thermalized neutrons have been evaluated, simulating the various phantoms placed against the collimator's mouth. Longitudinal profiles along the beam axis have been attained for each of the four phantoms. The results, reported in Fig. 4a, do not show significant differences of fluence in cubic and parallelepiped phantoms. In the spherical phantom, neutron thermalization appears shifted towards greater depths, as expected. Longitudinal profiles at various distances from the axis have been evaluated for the cubic phantom, and the results are reported in Fig. 4b.

The transversal profiles, reported in Fig. 5, are consistent with the results of Fig. 4 and give a easier visualization of the different lateral distribution of thermal neutron fluence. The differences, in fact, are not remarkable along the beam axis, with only a visible discrepancy for the spherical phantom. Out of the beam phantom, as expected, the fluence is affected by the lower width of the phantom itself and the consequent lack of return events from thermalized neutrons escaping from the phantom. Concerning the spherical phantom, there are greater differences due to the fact that neutrons enter in the phantom at distances from the collimator that grow with increasing the

distance from the beam axis. Note that in Fig. 5c for the depth of 0 cm only the central point is in contact with the phantom: the remaining curve represents the in-air fluence of thermalized neutrons and shows the distribution, along the collimator diameter, of the backscattered neutrons.

The fluence of neutrons with $E > 0.5$ eV has been calculated, along the beam axis, for the spherical, cubic and standard (40x40x20 cm^3) phantom. In the last two phantoms, fluences have resulted to be indistinguishable. A small difference was found in the spherical phantom, as seen in Fig. 6.

The gamma dose due to the 2.2 MeV photons emitted in the reactions of thermal neutrons with hydrogen has been calculated along the beam axis in three water phantoms: the standard phantom (40x40x20 cm^3), the cubic phantom (14 cm side) and the spherical phantom (16 cm in diameter). The results are reported in Fig. 7. The trends of the three profiles are easily justified. The trends of the profiles resulting in cubic and spherical phantoms show a trend that is partially correlated to the different distributions of the thermalized neutrons in the two phantoms, but a higher dose is observed in the cubic phantom. The dose in the standard phantom is significantly higher, while the profiles of the thermalized neutrons on the axis of the standard and cubic phantoms were very similar. This is due to the fact that the distances to which the photons carry energy are considerably longer than the paths of the thermal neutrons and then the contribution to the gamma dose due to photons emitted in the material that is absent in a smaller phantom is not negligible everywhere, even on the axis. In fact, the distribution of the mass around the beam axis in the cubic phantom is higher then that in the spherical, and the mass of the standard phantom is very higher.

Experimental results

Many experiments have been carried out at the LVR-15 research reactor. Measurements of neutron fluences and absorbed doses were performed with Fricke-gel dosimeters, thermoluminescence detectors (TLDs) and activation foils and the results are reported in previous papers. In particular, in some measurements [1,2] the absorbed dose and neutron fluence were measured in a cylindrical phantom (diameter16 cm, height 14 cm) placed against the collimator mouth of the LVR-15 epithermal column, with the cylinder axis on the beam axis. More recently, other measurements have been performed with the same phantom, but with the cylinder axis normal to the beam axis. The thermal neutron profiles along the beam axis have been achieved, in each experiment, by evaluating the absorbed dose due to the charged particles generated in the reactions with the isotope ^{10}B, introduced in suitable amount. As explained in the same previous paper [1], the absorbed dose in Gy for a ^{10}B concentration of 1 μg/g is related to the thermal neutron fluence Φ by the relation: $D = 8.63 \times 10^{-14} \times \Phi$. The thermal neutron profiles thus obtained have been verified by performing measurements, in the same irradiation configurations, with TLDs. The thermal neutron profiles along the beam axis obtained with the two different orientations of the phantom can be compared with the profiles of the thermalized neutrons evaluated, along the beam axis, for the cubic phantom and the spherical one. In both cases, we have two different irradiation geometries: (i) a configuration in which a plane surface of the phantom is placed against the collimator and (ii) a configuration in which a minimal part of the phantom is against the collimator mouth (a line for measurements with the cylindrical phantom and a point for calculations in a spherical phantom). In Fig. 8a, the thermal neutron profiles, obtained by the boron dose measured by means of gel dosimeters in the cylindrical phantom with the two different orientations, are show. In Fig. 8b, the profiles of thermalized neutrons in the cubic phantom and in the spherical one, obtained by MC simulations, are reported. It is evident the consistency between the obtained profiles. In fact, there is a remarkable analogy between the differences in the thermal neutron profiles resulting when the phantom surface against the collimator is flat and when it is not flat so that neutrons enter in the phantom at different distances from the collimator's mouth.

CONCLUSION

The here reported results give an idea of the spatial distribution of neutron fluence and gamma dose in water phantoms of different shapes and can be used to estimate the extent of changes that may occur by changing the shape and size of irradiated volume.

ACKNOWLEDGMENTS

REFERENCES
[1] Gambarini, G., Artuso,E., Giove, D., Volpe, L., Agosteo, S., Barcaglioni, L., Campi, F., Garlati, L., Pola, A., Durisi, E., Borroni, M., Carrara, M., Klupak, V., Marek, M., Viererbl, L., Vins, M., and d'Errico, F., "Fricke-gel dosimetry in epithermal or thermal neutron beams of a research reactor," Radiat. Phys. Chem., Vol. 116, 2015, pp. 21-27, http://dx.doi.org/10.1016/j.radphyschem.2015.03.025

[2] Gambarini, G., Artuso, E., Felisi, M., Colombo, G., Giove, D., Agosteo, S., Pola, A., Carrara, M., Klupak, V., Viererbl, L., Vins, M., Marek, M., "Gel Dosimeters for Dose Imaging in High Fluences of Epithermal Neutrons: Potentiality and Limitations", Nuclear Science Symposium and Medical Imaging Conference (NSS/MIC), 2015 IEEE, INSPEC Accession Number: 16356981, DOI: 10.1109/NSSMIC.2015.7581905.
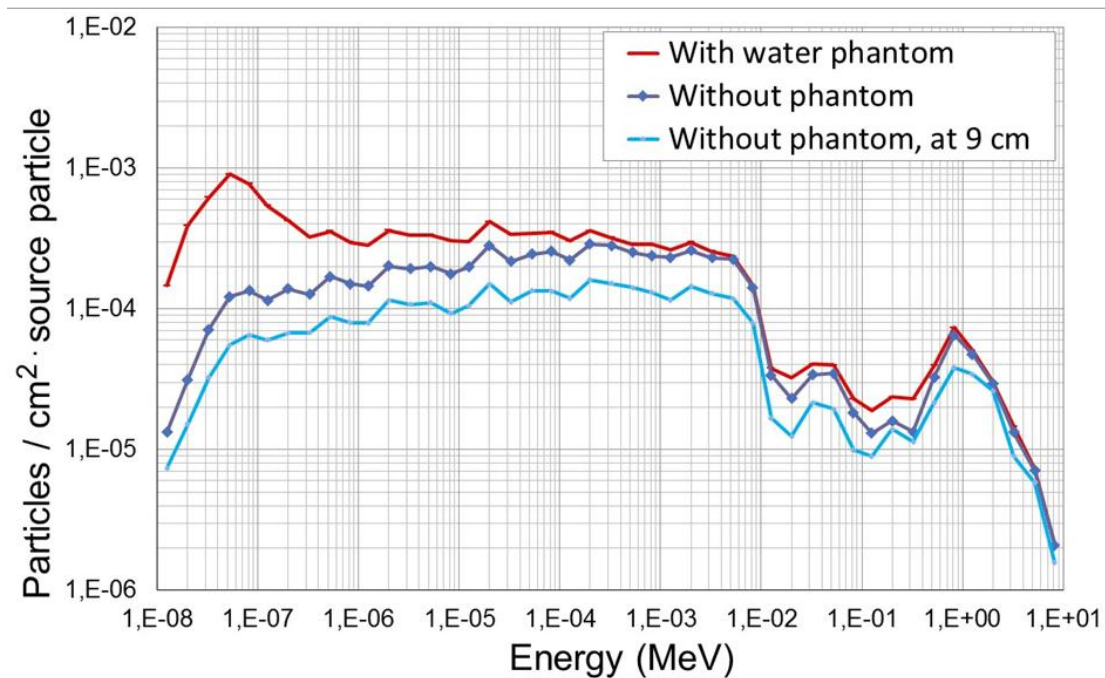
FIG. 1   Neutron energy spectra at the center of the collimator mouth, in absence of phantom (at the beam exit and at a distance of 9 cm, in air) and energy spectrum when a water phantom is placed against the collimator presence of a water phantom against the collimator.
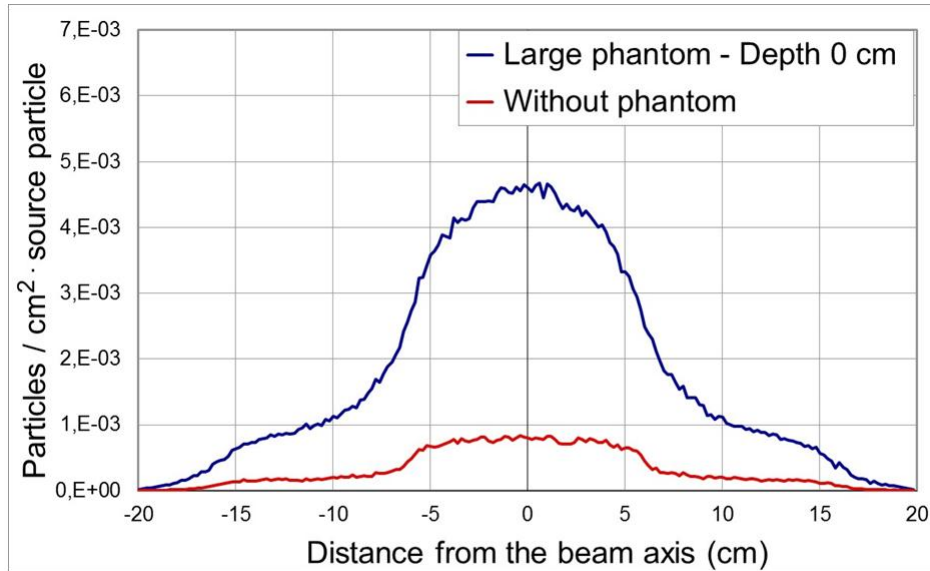
FIG. 2 Transversal profiles of the thermalized neutron fluence along a diameter of the collimator's mouth.
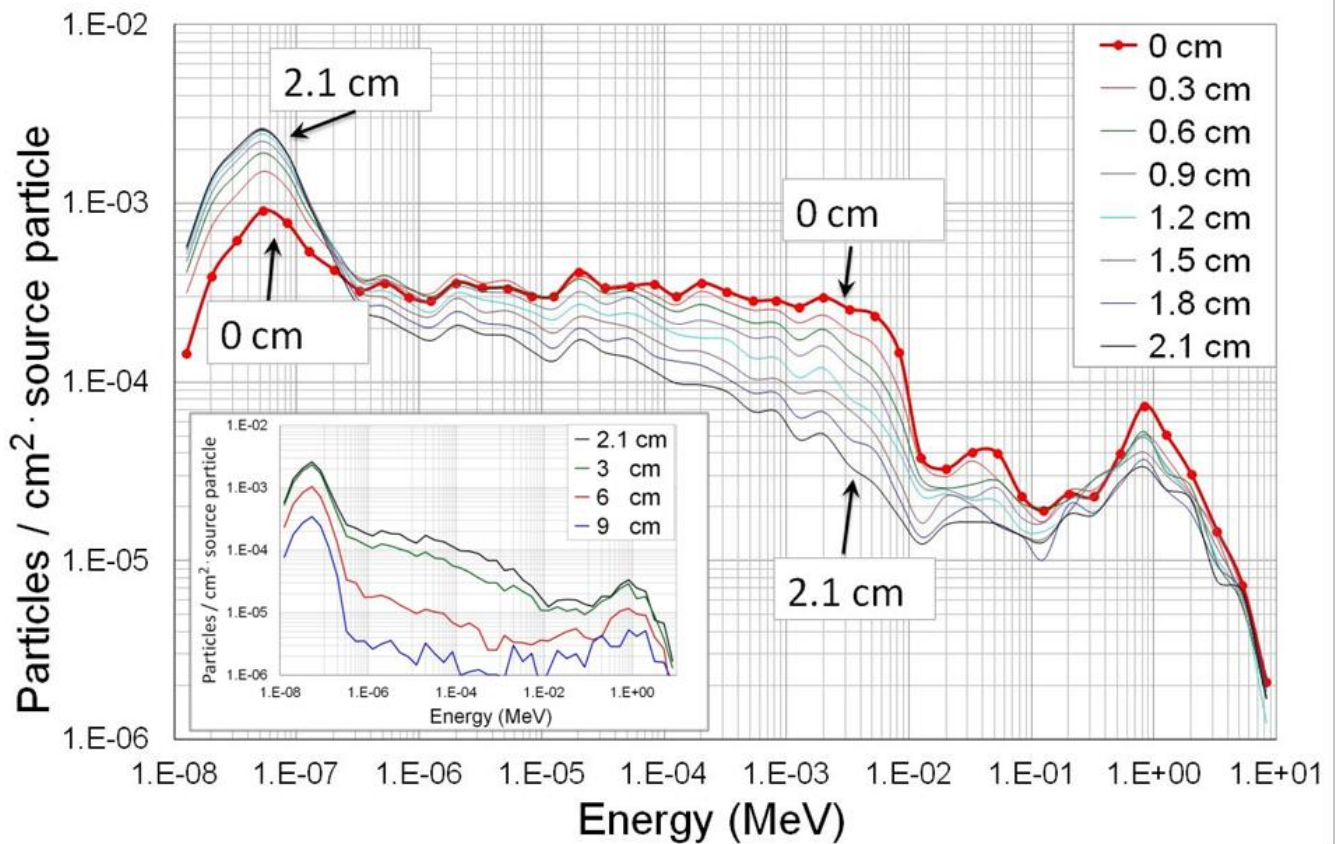

FIG. 3 Fluence spectra at depths in the cubic water phantom, from 0 cm to 2.1 cm. In the insert a few spectra from the same depth of 2.1 cm up to 9 cm are reported.
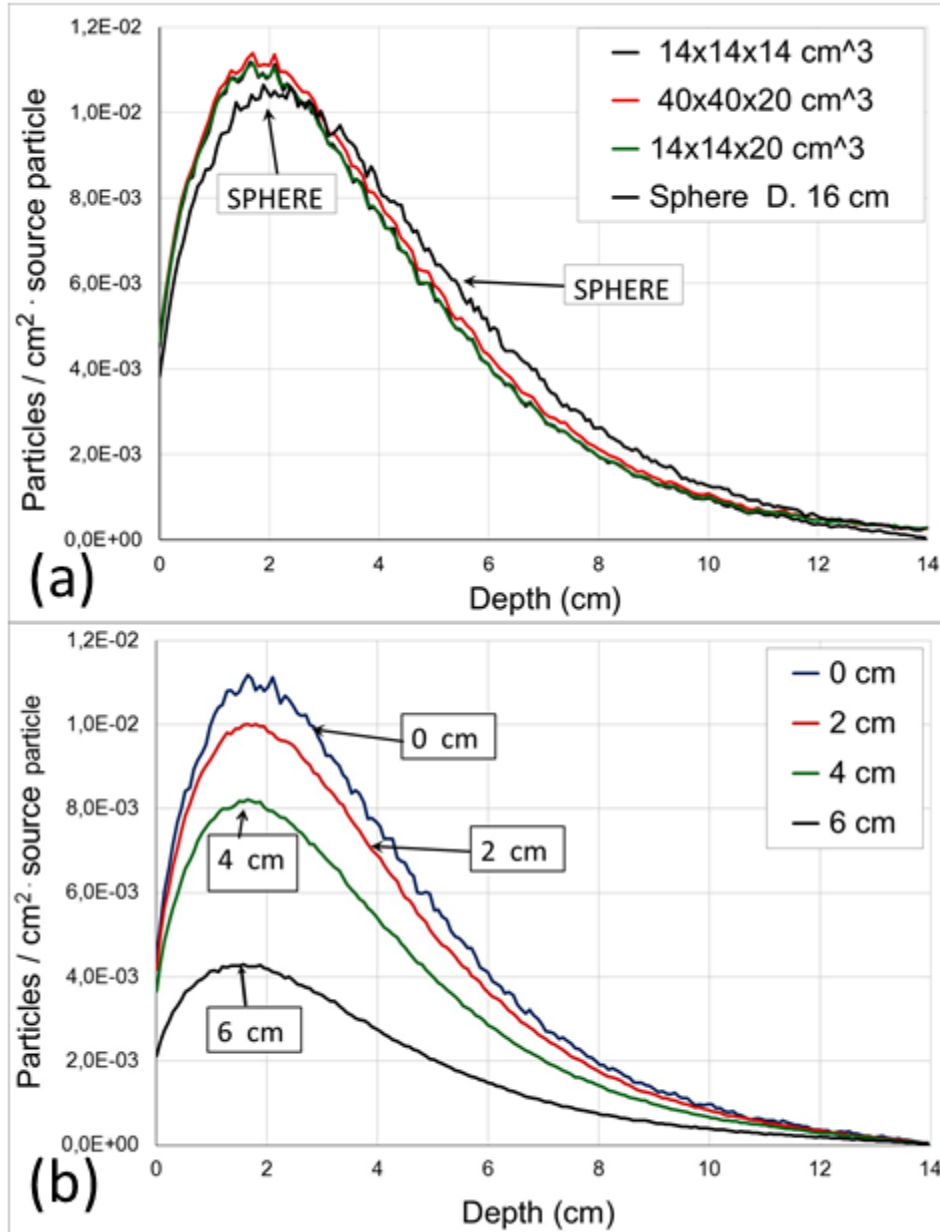
FIG. 4 (a) Longitudinal profiles of neutron fluence for E < 0.5 eV along the beam axis, evaluated for each of the four phantoms. (b) Longitudinal profiles of the same fluences at various distances from the beam axis, evaluated for the cubic phantom.
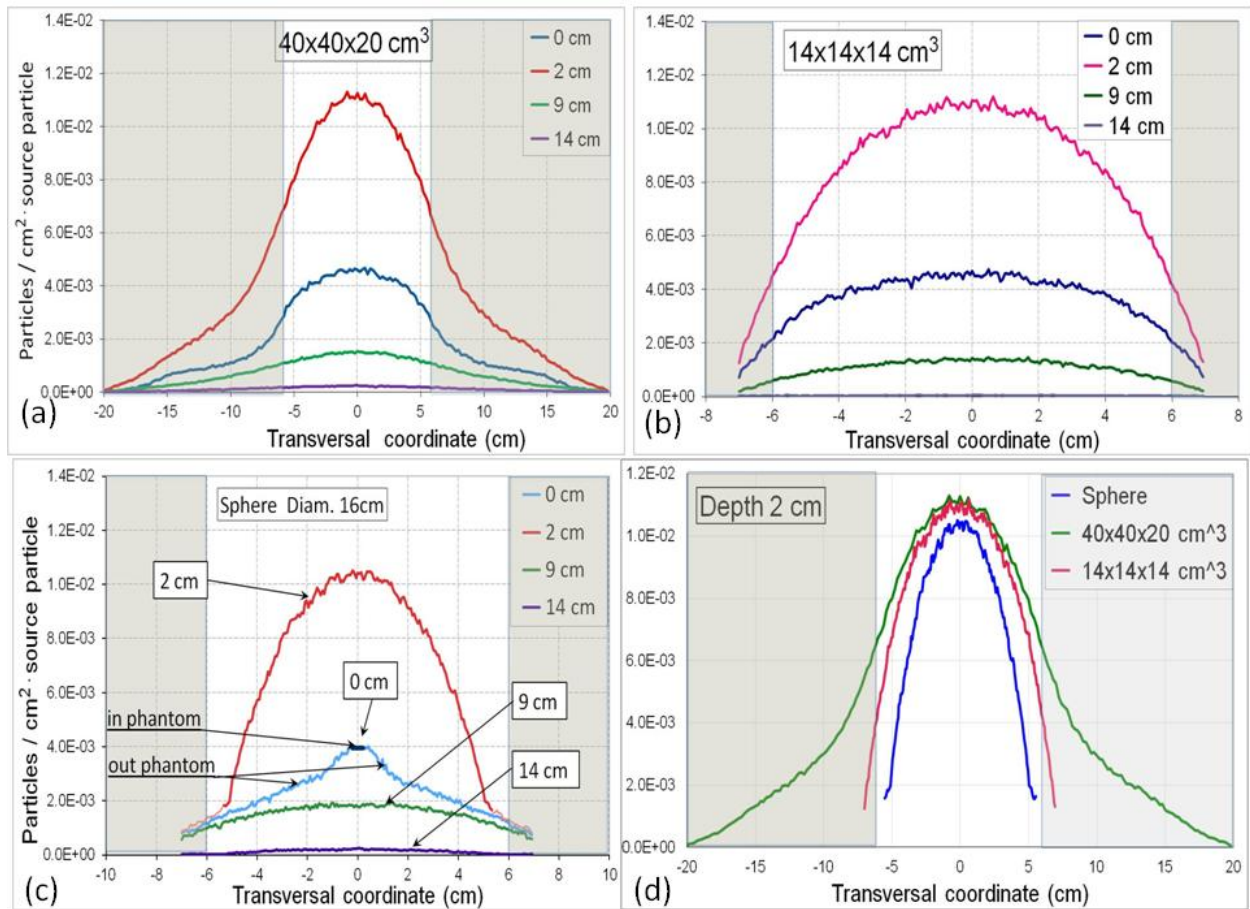
FIG. 5 (a), (b), (c) Transversal profiles of the fluence of neutrons with E < 0.5 eV at different depths in the various water phantoms: (a) standard (40x40x20 cm3), (b) cubic (14x14x14 cm3), (c) spheric (diameter 16 cm). (d) Transversal profiles of the fluence of neutrons with E < 0.5 eV at a depth of 2 cm in the three phantom, for easier comparison.
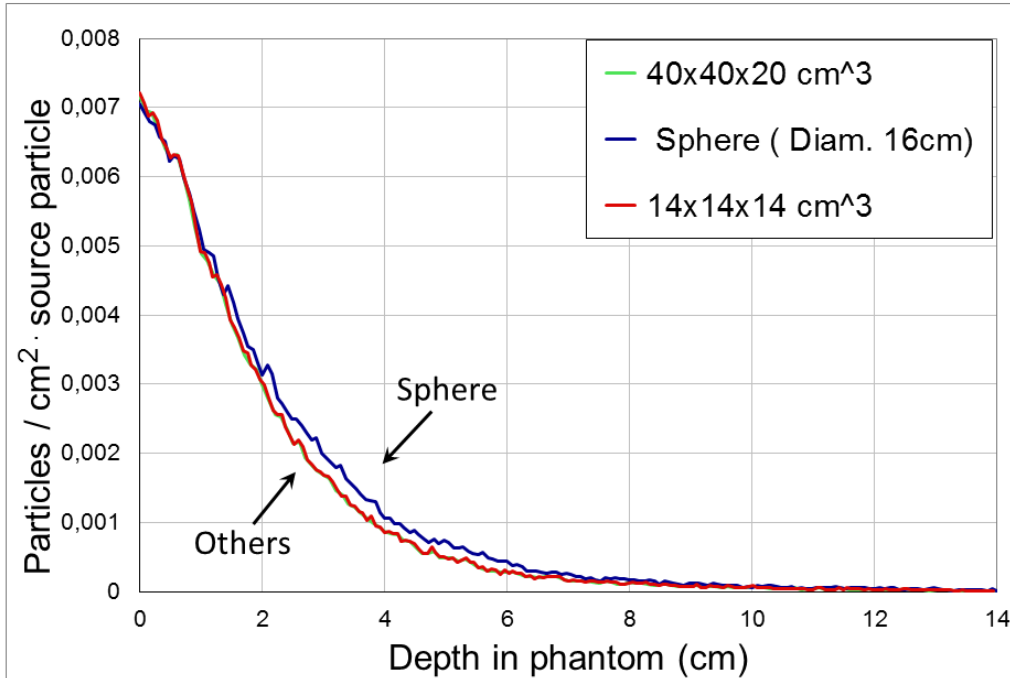
FIG. 6 Longitudinal profile of neutron fluence for E > 0.5 eV along the beam axis, evaluated for the same three phantoms of Fig. 5.
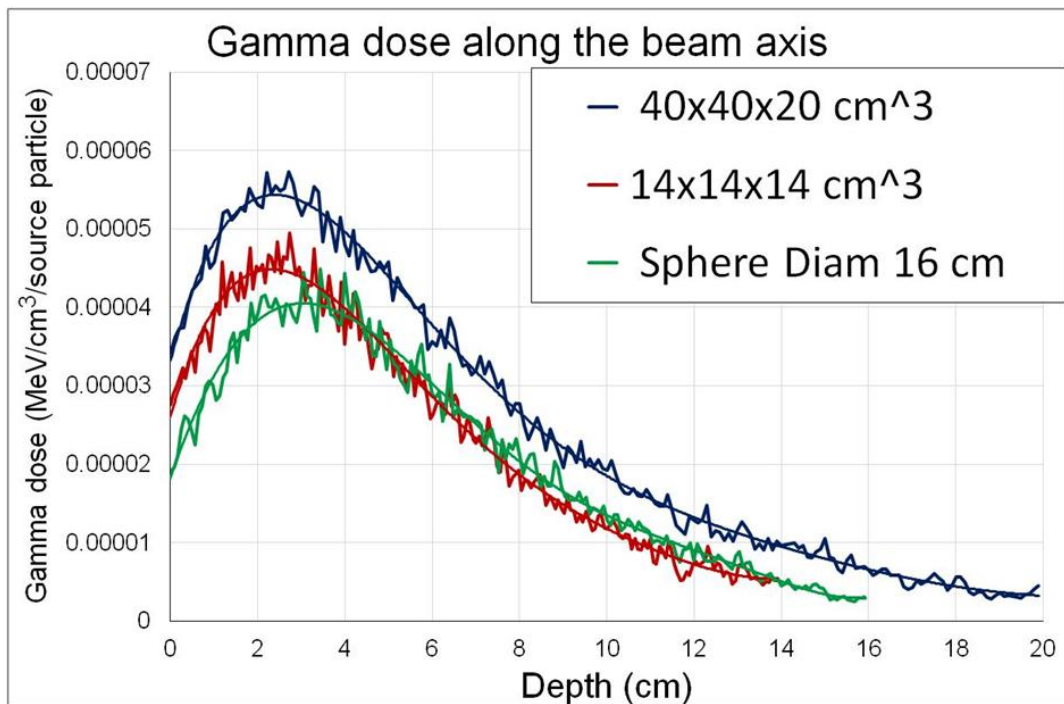

FIG. 7 Absorbed dose due to the 2.2 MeV photons emitted in the reactions of thermal neutrons with hydrogen, calculated along the beam axis of the same three phantoms of Fig. 5.
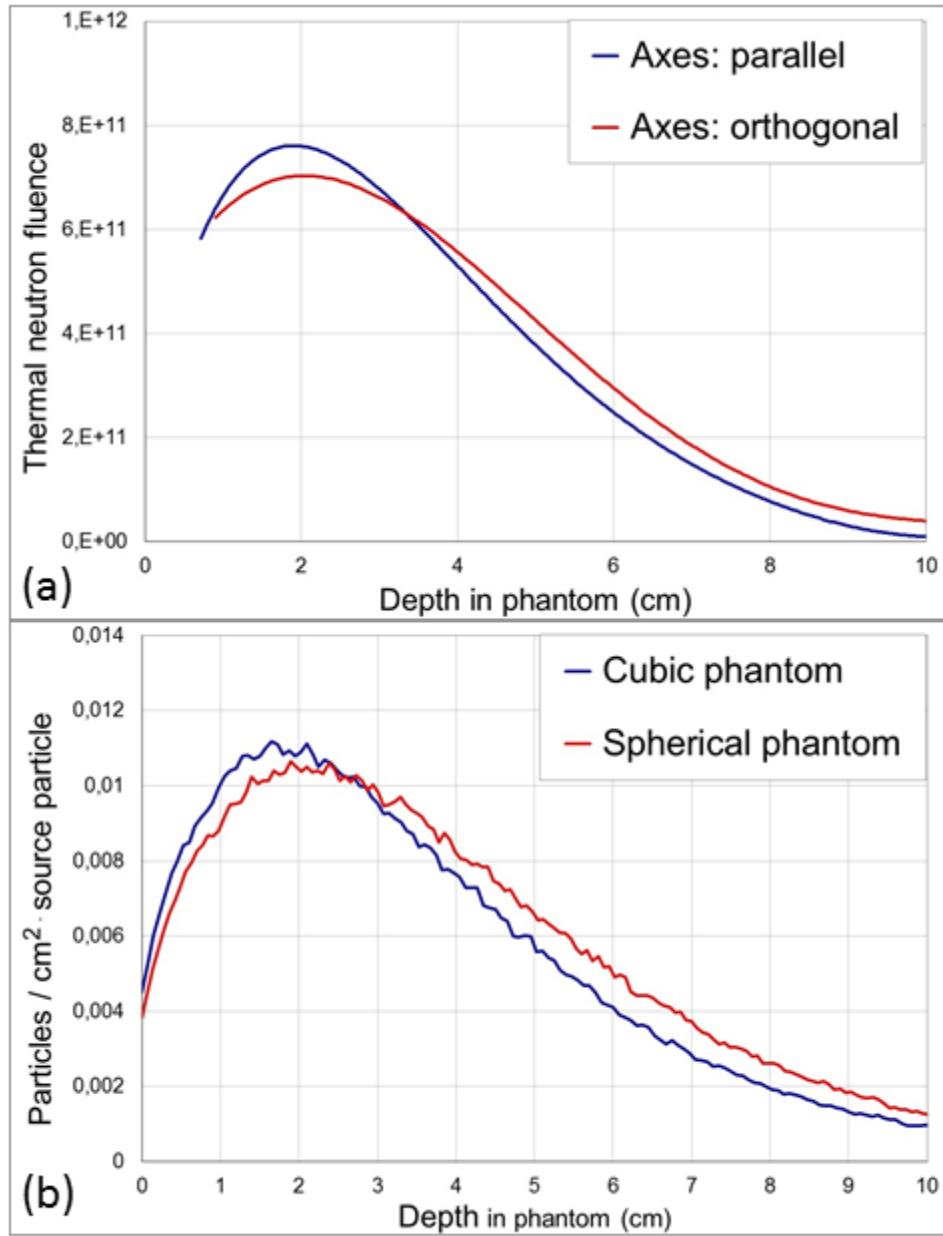
FIG. 8   (a) The thermal neutron profiles, obtained by the boron dose measured by means of gel dosimeters in a cylindrical phantom with two different orientations. (b) Profiles of thermalized neutrons in the cubic phantom and in the spherical one, obtained by MC simulations.